

## **Temperature-Dependent Adjustments of the Permafrost Thermal Profiles on the Qinghai-Tibet Plateau, China**

Authors: Changwei, Xie, Gough, William A., Lin, Zhao, Tonghua, Wu, and Wenhui, Liu

Source: Arctic, Antarctic, and Alpine Research, 47(4) : 719-728

Published By: Institute of Arctic and Alpine Research (INSTAAR), University of Colorado

URL: <https://doi.org/10.1657/AAAR00C-13-128>

---

BioOne Complete ([complete.BioOne.org](https://complete.BioOne.org)) is a full-text database of 200 subscribed and open-access titles in the biological, ecological, and environmental sciences published by nonprofit societies, associations, museums, institutions, and presses.

Your use of this PDF, the BioOne Complete website, and all posted and associated content indicates your acceptance of BioOne's Terms of Use, available at [www.bioone.org/terms-of-use](https://www.bioone.org/terms-of-use).

Usage of BioOne Complete content is strictly limited to personal, educational, and non - commercial use. Commercial inquiries or rights and permissions requests should be directed to the individual publisher as copyright holder.

---

BioOne sees sustainable scholarly publishing as an inherently collaborative enterprise connecting authors, nonprofit publishers, academic institutions, research libraries, and research funders in the common goal of maximizing access to critical research.

# Temperature-dependent adjustments of the permafrost thermal profiles on the Qinghai-Tibet Plateau, China

Xie Changwei<sup>1,3</sup>

William A. Gough<sup>2</sup>

Zhao Lin<sup>1</sup>

Wu Tonghua<sup>1</sup> and

Liu Wenhui<sup>1</sup>

<sup>1</sup>Cryosphere Research Station on the Qinghai-Tibet Plateau, State Key Laboratory of Cryospheric Sciences, Cold & Arid Regions Environmental and Engineering Research Institute, Chinese Academy of Sciences, Lanzhou, 730000, China

<sup>2</sup>Department of Physical & Environmental Sciences, University of Toronto-Scarborough, Toronto, ON, M1C 1A4, Canada

<sup>3</sup>Corresponding author: xiecw@lzb.ac.cn

## Abstract

Using continuous data obtained from 17 monitoring sites, the permafrost temperature profiles and the depths of zero annual amplitude (DZAA) on the Qinghai-Tibet Plateau are examined. Permafrost thermal trumpet curves are generally narrow and the DZAAs are generally shallow in warm permafrost regions, especially at sites where the permafrost temperature is close to 0 °C. The observed DZAAs in warm permafrost regions are indeed generally less than 7.0 m and for three sites less than 4.0 m. In low-temperature permafrost areas, the situation is reversed: the thermal trumpet curves are generally wide and the DZAAs are generally deep. Theoretical and numerical analyses clearly show there is a causal relationship between permafrost warming and the decrease of the DZAA. Latent heat effects are buffering the increase of permafrost temperature and result in narrow thermal trumpet curves and shallow DZAAs. Based on observations and numerical analyses, this research suggests that most of the permafrost on the Qinghai-Tibet Plateau is undergoing internal thaw and the latent heat effects have important implications on the permafrost thermal regime. The temperature-dependent adjustments in permafrost will promote both the downward and upward degradation of permafrost as a result of climate warming.

DOI: <http://dx.doi.org/10.1657/AAAR00C-13-128>

## Introduction

Nearly universal warming of permafrost across the polar northern hemisphere in the past several decades has been observed (Lemke et al., 2007; Christiansen et al., 2010; Romanovsky et al., 2010a, 2010b; Smith et al., 2010). However, there is a large variation in the magnitude of permafrost temperature change within these permafrost regions. Permafrost with lower temperatures (<−2.0 °C) is warming more rapidly, especially in the Northern Arctic. In northern Alaska, northern Europe, Russia, and at Alert on Ellesmere Island in northern Canada, recorded warming rates near or above 0.1 °C yr<sup>−1</sup> in the past several decades have been reported (Oberman and Mazhitova, 2001; Osterkamp, 2003; Hinzman et al., 2005; Walsh et al., 2005). Warming rates are weaker for permafrost with higher temperatures in lower latitudes, especially for permafrost already at temperatures close to 0 °C. For this warm permafrost, latent heat effects dominate the ground thermal regime and mitigate the rate of temperature change (Romanovsky et al., 2010a). In the interior of Alaska, where permafrost is warmer than that in northern Alaska, permafrost temperatures have increased by 0.5–1.5 °C from 1983 to 2003, about half of the rate of northern Alaska (Osterkamp, 2005). On the Qinghai-Tibet Plateau (QTP), where the highest and most extensive high altitude permafrost on Earth is located (Cheng and Wu, 2007), observations indicate that at sites with long-term mean permafrost temperature at or above −1.0 °C, the rate of permafrost temperature increase was usually less than 0.3 °C 10 yr<sup>−1</sup>, whereas at sites with long-term mean permafrost temperature lower than −2.0 °C, the rate of permafrost temperature increase was greater than 0.5 °C 10 yr<sup>−1</sup> during the 1996–2006 period (Wu and Zhang, 2008).

In contrast, the magnitude of active-layer thickness (ALT) increase is greater in warm permafrost regions than in cold permafrost regions. Over Alaska and northern Canada, cold permafrost

regions, there is evidence of large interannual variations of ALT but no significant trend since the early 1990s (Brown et al., 2000; Nelson et al., 2004; Smith et al., 2009; Wu and Zhang, 2010). In Siberia, another cold permafrost region, the average magnitude of ALT has increased only about 21 cm from the early 1960s to 2000 (Frauenfeld et al., 2004; Zhang et al., 2005; Wu and Zhang, 2010). However, on the QTP, the average rate of the ALT increase is about 5.0 cm yr<sup>−1</sup> in cold permafrost regions, whereas in warm permafrost areas, the mean rate of increase is as much as 11.2 cm yr<sup>−1</sup> from 1995 to 2007 (Wu and Zhang, 2010). In Mongolia, the largest rates of increase of ALT of 20–40 cm yr<sup>−1</sup> were observed during the past decade at those boreholes where the mean annual ground temperature was close to 0 °C and a smaller rate of increase usually occurred in shallow active layers over ice-rich and colder permafrost (Zhao et al., 2010).

Permafrost temperature conditions not only have important implications for the warming trend of the permafrost, but also have significant implications on the distribution of ground and subsurface temperatures. In warm permafrost regions, the permafrost temperature profiles are highly sensitive to varying soil thermal properties (Smith and Riseborough, 1985; Riseborough, 1990). Recently, the characteristics of the ground temperature profiles of permafrost within different temperature regimes have been reported in the literature (Lemke et al., 2007; Christiansen et al., 2010; Romanovsky et al., 2010a, 2010b; Smith et al., 2010; Zhao et al., 2010). The focus is largely on the influence of related factors such as snow cover and vegetation while some researchers have suggested that the latent heat effects have significant implications on the thermal profiles (e.g., Romanovsky et al., 2010a; Smith et al., 2010). Generally, the thermal regime of deep permafrost is a conservative realm and has a long response time and reacts to climatic fluctuations slowly. Disturbance of temperature distribution at depth always requires several years or decades for permafrost to re-

spond to atmospheric warming or cooling (Haerberli et al., 1993). It is not possible to fully assess the rate of change of ground temperature distribution at the monitoring sites since long-term observation is still in its infancy. However, the causal relationship between the permafrost thermal regime and changes in thermal characteristics can be explored through analysis of permafrost data already collected from different thermal regimes as well as by theoretical and numerical analyses. In this study, we explored the temperature profiles and the depths of zero annual amplitude (DZAA) of 17 monitoring sites on the QTP using continuous data obtained from 2006 to 2010. We analyzed the characteristics of the permafrost thermal regime at different sites with different temperature. In the discussion part of this paper, the causal relationship between permafrost thermal conditions and decrease of the DZAA is presented through theoretical and numerical analyses. The aim of this study is to analyze how the permafrost thermal regime of the QTP has adjusted to the change of soil temperature and what factors influence this adjustment.

## Methods and Data

During the past several decades, permafrost has been increasingly studied on the QTP (Fig. 1). Most of the studies are concentrated along the Qinghai-Xizang Highway (QXHW) and the Qing-Kang Highway due to the region's isolation and harsh environmental conditions in the hinterland of the QTP (Cheng and Wu, 2007; Jin et al., 2008; Wu et al., 2010a; Zhao et al., 2010; Xie et al., 2012). Thousands of boreholes were drilled into the permafrost for the engineering design and construction of the Qinghai-Xizang Railway and for scientific research programs. Since the 1980s, an integrated permafrost monitoring network including more than 20 boreholes with depths from 20 to 127 m has been set up along

the QXHW (Cheng and Wu, 2007; Zhao et al., 2010; Xie et al., 2012). All the boreholes are located at least 2 to 5 km away from the highway in order to avoid the direct influence of the QXHW. Thermistor sensors were installed on cables and were permanently installed into these boreholes, which were cased using 5 cm diameter steel pipes (Zhao et al., 2010). Generally, the thermistor sensors were deployed at 1 m intervals near the surface ( $\leq 6-8$  m) and 2-3 m intervals at deeper depths. These thermistor sensors, which were made at the Chinese State Key Laboratory of Frozen Soil Engineering at Lanzhou, have excellent sensitivity ( $\pm 0.01$  °C) in laboratory tests (Cheng and Wu, 2007). Initially, soil temperatures at different levels were measured three times per month by hand and then averaged over a year. Automated data-loggers have been subsequently installed to record temperatures and water content at various horizons in the active layer since 1998 and have been commonly used to record ground temperatures at different depths in permafrost since 2005. At the present time, all sites are equipped with Campbell Scientific data-loggers (model CR10X, CR1000, or CR3000) to record the measurements (Zhao et al., 2010).

Soil temperature data used in this study were obtained from 17 monitoring boreholes along the QXHW during the 2006 to 2010 period (Fig. 2). Permafrost temperatures in all of these boreholes are automatically recorded 12 times per day at 2-hour intervals during the study period. Tables 1 and 2 summarize geographical locations, soil type, vegetation cover, permafrost conditions, and monitoring period at each site. The soil types are observed near the surface and varied from fine materials as clay to silt/sand/gravel, consistent with Wu and Zhang (2008, 2010). At some sites, soil temperature and water content were both monitored at many horizons in the active layer, such as XDT, QTB02, QTB09, QTB16, and QTB18.

In this study, meteorological data are collected from three automated weather stations (AWS) that are located in Xidatan,

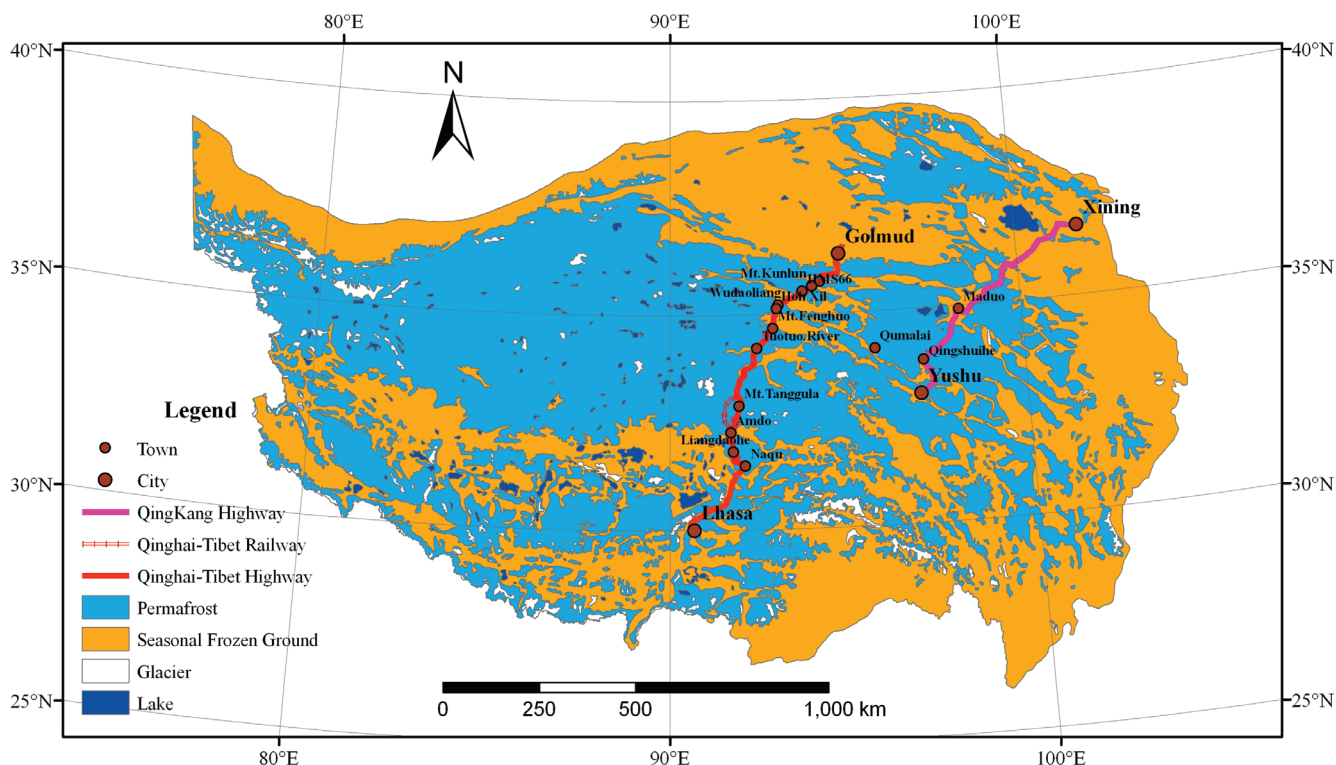
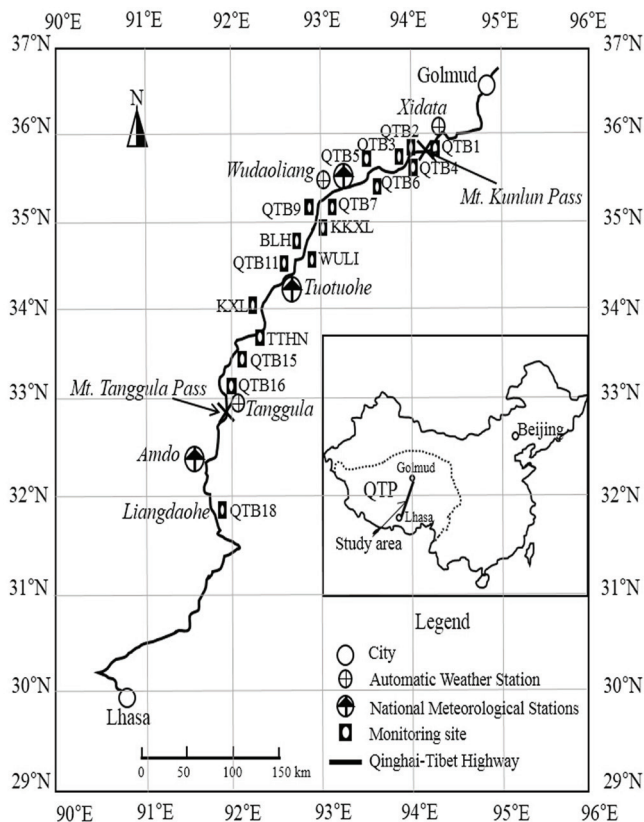


FIGURE 1. Map of permafrost distribution on the Qinghai-Tibet Plateau (QTP) (adapted from Cheng and Wu, 2007).



**FIGURE 2.** The locations of 17 monitoring sites along the Qinghai-Xizang Highway (QXHW) on the QTP.

Wudaoliang, and Tanggula (Fig. 2). Air temperature and precipitation have been continuously observed at these three meteorological stations during the study period. Long-term meteorological data are provided by three Chinese National Meteorological Stations (CNMS), which are located in Wudaoliang, Tuotuohe, and Amdo. In addition, air temperature was also observed at 0.5 m above the surface at these monitoring sites (boreholes) during the study period. Thus, for each of the permafrost monitoring sites in this study, the air temperature can be obtained either locally or from nearby weather stations.

#### PERMAFROST THERMAL STATE AND THERMAL PROFILES

Geographically, spatial patterns of permafrost temperature distribution on the QTP are controlled by regional zonations of elevation, latitude, and continentality (Cheng, 1983; Zhou et al., 2000; Jin et al., 2008; Wu et al., 2010b) and are significantly affected by local environmental factors such as vegetation, snow cover, soil water content, and geological landform (Cheng, 2003; Wang et al., 2002; Jin et al., 2008; Lu et al., 2008; Pang et al., 2011). Recently, the main characteristics of permafrost conditions, the recent permafrost warming, and the changes in the active layer were discussed in detail by Cheng and Wu (2007), Wu and Zhang (2008, 2010), Wu et al. (2010a, 2010b), Zhao et al. (2010), and Xie et al. (2012). Therefore, in this study, we only focus on the characteristics of the thermal profiles at these monitoring sites.

Figure 3 shows the permafrost temperature (the mean annual ground temperature at the depth of zero annual amplitude [DZAA, Qiu et al. 1994]) at all the 17 monitoring sites along the QXHW. Eleven permafrost sites are classified as warm permafrost, which

**TABLE 1**  
Geographical data and information of 17 monitoring sites on the Qinghai-Tibet Plateau (QTP).

Sites	Location		Areas	Altitude (m)	Established time	Daily data available
	Latitude	Longitude				
QTB1	35°42'56"N	94°04'56"E	Xidatan	4230	1990.10	2006.01–2010.12
QTB2	35°37'32"N	94°03'34"E	Mount Kunlun	4753	1990.10	2006.01–2010.12
QTB3	35°31'23"N	93°47'04"E	66Daoban	4560	1990.10	2006.01–2010.12
QTB4	35°25'50"N	93°36'01"E	Qinshuihe 203	4488	2005.10	2006.01–2010.12
QTB5	35°21'51"N	93°26'47"E	Chumaer River	4520	2005.10	2006.01–2010.12
QTB6	35°17'24"N	93°16'08"E	Hoh Xil Bridge	4563	2005.10	2006.01–2010.12
QTB7	35°11'36"N	93°04'26"E	Wudaoliang	4656	1990.10	2006.01–2010.12
QTB9	35°08'19"N	93°02'28"E	Hoh Xil	4804	2007.10	2006.01–2010.10
KKXL	35°07'59"N	93°01'59"E	Hoh Xil	4740	2005.10	2006.01–2010.12
BLH	34°49'46"N	92°55'57"E	Beilu River	4621	2002.10	2008.12–2010.10
WULI	34°28'39"N	92°43'33"E	Wuli	4571	2007.06	2008.12–2010.10
QTB11	34°23'13"N	92°39'22"E	Wuli	4623	2005.10	2006.01–2010.12
KXL	33°57'21"N	92°20'18"E	Kaixinlin	4726	2002.10	2006.01–2010.10
TTHN	33°46'23"N	92°14'05"E	Tongtian River	4886	2005.10	2006.01–2010.10
QTB15	33°05'51"N	91°53'52"E	Wenquan	4960	2005.10	2006.01–2010.12
QTB16	33°04'19"N	91°56'19"E	Tanggula	5100	2006.10	2006.07–2010.12
QTB18	31°49'07"N	91°44'12"E	Liangdaohe	4808	1975.10	2006.01–2010.12

Note: dates are given in the form yyyy.mm.

**TABLE 2**  
**Climatic and environmental parameters at 17 monitoring sites on the QTP.**

Sites	Climate conditions		Permafrost conditions				Site descriptions
	MAAT (°C)	Precipitation (mm)	ALT (m)	DZAA (m)	MAGT (°C)	PT (m)	
QTB1	-2.0 to -4.5	300-350	1.65	6.4	-0.45	21.0	Sandy clay, flat surface, alpine grasslands
QTB2	-5.5 to -6.5	250-300	1.50	7.4	-2.25	—	Sandy clay, gentle slope, alpine grasslands
QTB3	-3.5 to -5.5	250-300	3.31	3.8	-0.41	—	Desertification surface, alpine grasslands
QTB4	-3.0 to -4.5	250-300	1.82	3.3	-0.35	20.0	Sandy clay, flat surface, alpine meadow
QTB5	-3.0 to -4.5	250-300	8.30	7.7	-0.03	5.2	Desertification surface, alpine grasslands
QTB6	-3.0 to -4.5	250-300	3.32	3.9	-0.47	32.0	Sandy clay, flat surface, alpine grasslands
QTB7	-3.5 to -4.5	250-300	1.55	6.8	-1.53	—	Sandy clay, flat surface, alpine meadow
QTB9	-3.5 to -5.0	300-350	1.35	10.2	-2.70	—	Silt, clay, flat surface, alpine meadow
KKXL	-3.5 to -5.0	300-350	1.58	10.3	-2.54	—	Sandy clay, flat surface, alpine meadow
BLH	-2.5 to -4.5	250-350	2.10	6.8	-0.34	21.5	Silt, clay, flat surface, alpine meadow
WULI	-2.8 to -4.0	250-350	3.32	6.3	-0.45	24.0	Sandy clay, flat surface, alpine grasslands
QTB11	-2.8 to -4.0	250-350	2.71	14.9	1.90	—	Desertification surface, alpine grasslands
KXL	-3.0 to -5.0	250-350	2.74	6.5	-0.55	—	Sandy clay, gentle slope, alpine grasslands
TTHN	-3.0 to -5.0	250-350	2.80	6.5	-0.48	26.5	Sandy clay, flat surface, alpine meadow
QTB15	-3.5 to -5.0	250-350	2.35	14.5	-1.03	—	Gravel and sandy, alpine grasslands
QTB16	-4.0 to -5.5	300-350	3.15	17.4	-1.25	—	Gravel, silt, gentle slope, alpine grasslands
QTB18	-1.8 to -2.5	350-450	1.25	8.2	-0.73	—	Clay, flat surface, alpine meadow

MAAT: mean annual air temperature; ALT: active layer thickness; DZAA: the depths of zero annual amplitude; MAGT: mean annual ground temperature at the DZAA; PT: permafrost thickness.

is defined as permafrost temperature at or higher than  $-1.0\text{ }^{\circ}\text{C}$  (Wu and Zhang, 2008; Wu et al., 2010a), and eight of them are warmer than  $-0.5\text{ }^{\circ}\text{C}$ . Warm permafrost is widely distributed in Xidatan basin, Chumaer River basin, Tuotuohe River basin, and in the south of Tanggula Mountains. Permafrost with temperature below  $-2.0\text{ }^{\circ}\text{C}$  was only found at three sites, QTB2, QTB9, and KKXL. QTB2

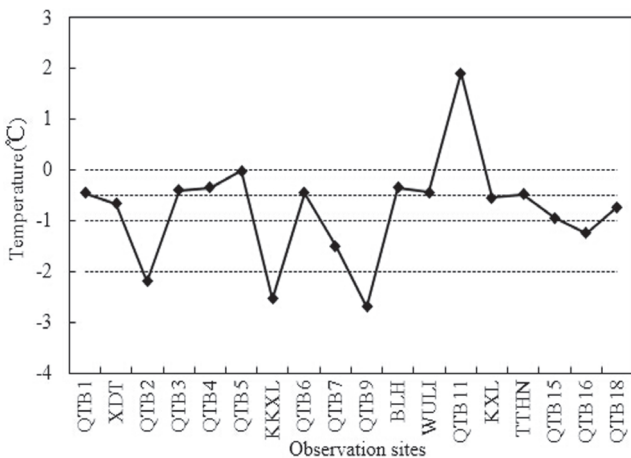


**FIGURE 3. Permafrost temperatures (the mean annual ground temperature at the depth of zero annual amplitude [DZAA] in 2010) at 17 monitoring sites along the QXHW.**

is located at the south-facing slope of Kunlun Mountains, and both QTB9 and KKXL are located in the Hoh Xil Mountains.

In permafrost regions, as the air temperature oscillates through its annual cycle, the ground temperature will reflect these temperature changes to a certain depth and with a time lag. The minimum and maximum temperature of the soil form trumpet curves that intersect at the DZAA, where annual temperature variations cease. These annual trumpet curves can be used to characterize the ground thermal regime of the permafrost (Smith et al., 2009). From Figure 4, it can be seen that the shape of the thermal trumpet curves varies considerably among the 17 monitoring sites. The thermal trumpet curves are usually narrow at the sites with permafrost temperature close to  $0\text{ }^{\circ}\text{C}$  (warm permafrost), while they are wider at the cold-permafrost sites. For example, at QTB5 the permafrost is found at depths between  $-8.3\text{ m}$  and  $-13.5\text{ m}$  and permafrost temperature is  $-0.03\text{ }^{\circ}\text{C}$ . The ground temperature in the permafrost remains stable throughout the year while they change dramatically in the unfrozen soil. Similarly, at QTB1, where permafrost temperature is  $-0.43\text{ }^{\circ}\text{C}$ , the amplitude of ground temperature in the upper section (above the DZAA, 3.9 m) of permafrost attenuates rapidly from  $34.5\text{ }^{\circ}\text{C}$  at the surface to  $0.1\text{ }^{\circ}\text{C}$  at the DZAA, and the maximum temperature gradient is larger than  $5.0\text{ }^{\circ}\text{C m}^{-1}$  in winter. In the lower section (from the DZAA to the bottom of the permafrost), the amplitude of ground temperature is close to  $0\text{ }^{\circ}\text{C}$ . Similar thermal trumpet curves can be found at other warm permafrost sites such as QTB3, QTB4, QTB6, BLH, WULI, KXL, and TTHN. Permafrost temperatures at all of these sites are higher than  $-0.6\text{ }^{\circ}\text{C}$ .

In cold permafrost regions, in contrast, permafrost usually extends deeper than the drilling depths and the fluctuations of air

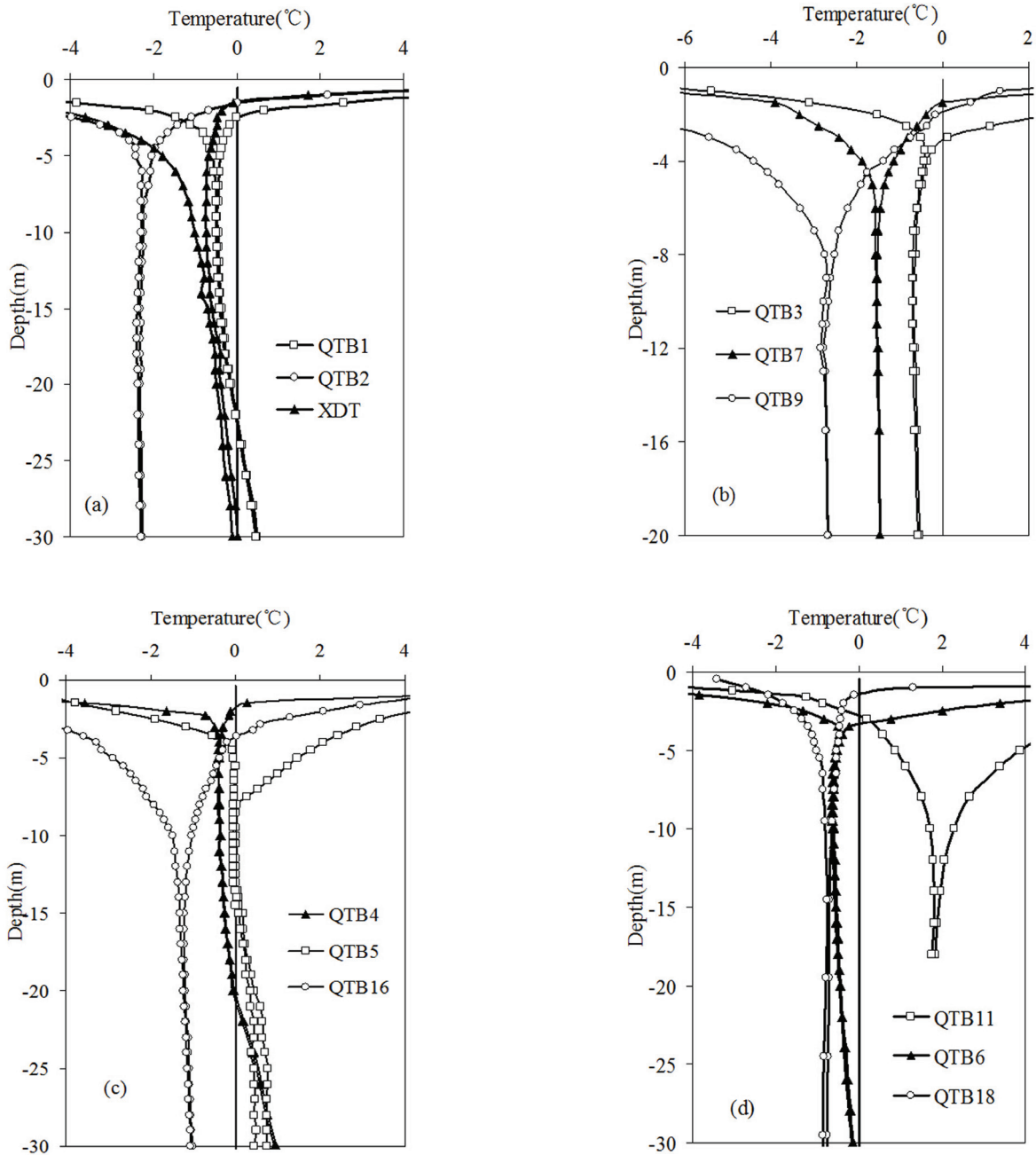


FIGURE 4. The thermal trumpet curves of ground temperature at some monitoring sites in 2010 (ground temperature using the same proportion).

temperature can be transferred into deeper horizon. For example, at QTB9, where the permafrost temperature is  $-2.74\text{ }^{\circ}\text{C}$ , the annual amplitude of the ground temperature is attenuated slowly with depth and the temperature gradients within the deep drilling depths are close to  $0\text{ }^{\circ}\text{C m}^{-1}$ . Similar thermal trumpet curves can be found at KKXL, QTB15, and QTB16 where permafrost temperatures are below  $-1.0\text{ }^{\circ}\text{C}$ . Wide thermal trumpet curves are also found at QTB11, which is the only site that is located in a nonpermafrost region. The shape of the thermal trumpet curve is strikingly different from WULI, although both sites are located in the same region. These characteristics of the thermal trumpet curves imply that temperature regime, cold or warm, has important implications for the temperature profile of permafrost.

#### PERMAFROST THERMAL STATE AND THE DZAA

The temperature at the DZAA is usually considered as the mean annual temperature of permafrost. Normally, the operational definition for the DZAA is the depth where the change of measured temperature is less than  $0.1\text{ }^{\circ}\text{C}$  annually (Williams and Smith, 1989). This operational definition is widely used in spite of higher thermistors' accuracy (e.g., Zhou et al., 2000; Isaksen et al., 2007; Burn and Zhang, 2009; Smith and Brown, 2009). DZAA can be used as a metric to assess the influence of the temperature regime and other factors on the permafrost thermal profile.

Figure 5 shows the DZAA for the 17 sites along the QXHW in 2010. The DZAA at more than half the monitoring sites is less



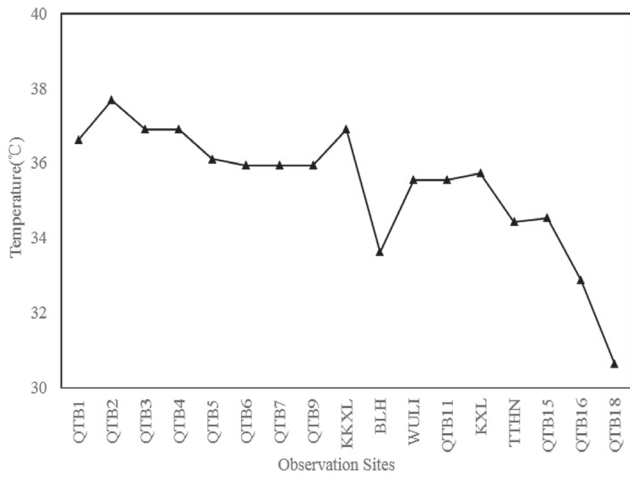


**FIGURE 7. Annual air temperature amplitudes at the 17 monitoring sites in 2010 along the QXHW.**

the QXHW, because the DZAAs do not follow the same distribution pattern. Snow cover may have an important influence on permafrost temperature. Generally, though, there is relatively little snow on the ground in winter on the QTP (Wu and Zhang, 2008). Snow cover is an efficient buffer layer that can significantly retard the seasonal and interannual fluctuations of heat transfer into the ground (Goodrich, 1976; Williams and Smith, 1989; Romanovsky et al., 2010b). Similarly, it can be inferred that snow cover does not have significant influence on the distribution of the DZAA along the QXHW, as the DZAA is usually deep at the sites located in high mountains, where the seasonal snow cover is thick, while it is shallow at the sites located in low regions, where the seasonal snow cover is thin.

From the observations reported in this paper, it can be found that permafrost thermal profiles along the QXHW are primarily determined by the soil temperature regime although the specific regional settings have important implications. However, it is difficult to investigate the temporal trend of ground temperature distribution at specific monitoring sites and the relationship between soil temperature and permafrost profiles, on the one hand because the long-term observation is still in its infancy, and on the other hand because the environmental setting has important thermal influences. In this section, we discuss the temperature-dependent adjustments of the thermal profile in permafrost through theoretical and numerical analyses.

For permafrost, the general features of the thermal regime that experiences annual variations, such as the exponential attenuation of seasonal temperature amplitude with depth and associated lag in phase, can be analyzed using the heat conduction equation with a sinusoidal surface temperature variation (Williams and Smith, 1989). If the geothermal gradient term is ignored, the temperature at any depth,  $z$ , can be calculated by the following (Williams and Smith, 1989):

$$T(z, t) = \bar{T}_z + A_s e^{-z(\omega/2\kappa)^{1/2}} \sin \left[ \omega t - \left( \frac{\omega}{2\kappa} \right)^{1/2} z \right] \quad (1)$$

where  $\kappa$  is the soil thermal diffusivity ( $\text{m}^2 \text{s}^{-1}$ );  $\omega = 2\pi P^{-1}$ ,  $P$  is the period of the wave (1 year), and  $A_s$  is the amplitude of the surface temperature wave. Time  $t$  is counted from the date in spring

when the surface temperature wave passes through its mean annual value. The expression

$$A_z = A_s e^{-z(\omega/2\kappa)^{1/2}} = A_s e^{-z(\pi/\kappa P)^{1/2}} \quad (2)$$

represents the amplitude of the temperature wave at depth  $z$ . As introduced previously, the DZAA is the distance from the surface to the depth beneath which there is virtually no annual fluctuation in ground temperature (Williams and Smith, 1989). It can also be defined as the depth where the annual wave is delayed by exactly 1 year from that at surface (Williams and Smith, 1989). This is given by

$$DZAA = 2(\pi\kappa P)^{1/2}. \quad (3)$$

In a saturated system, thermal diffusivity, thermal conductivity, and the volumetric heat capacity for a mixture of soil particles, unfrozen water, and ice are represented as (Williams and Smith, 1989; Xu et al., 2001):

$$\kappa = \frac{\lambda}{C} \quad (4)$$

$$\lambda \approx \lambda_w^{W_u} \cdot \lambda_i^{W_i} \cdot \lambda_m^{1-W} \quad (5)$$

$$C = C_f + L \cdot \rho_d \cdot \frac{\partial W_u}{\partial T} \quad (6)$$

$$C_f = C_{sf} + (W - W_u)C_i + W_u C_u \quad (7)$$

$W$  is the total water content;  $\lambda$ ,  $\lambda_w$ ,  $\lambda_i$ ,  $\lambda_m$  are the thermal conductivity of the frozen soil, unfrozen water ( $0.55 \text{ W m}^{-1} \text{ }^\circ\text{C}^{-1}$ ), ice ( $2.22 \text{ W m}^{-1} \text{ }^\circ\text{C}^{-1}$ ), and minerals;  $C$ ,  $C_f$ ,  $C_{sf}$ ,  $C_i$ , and  $C_u$  are the heat capacity of frozen soil, sensible heat capacity of the frozen soil, minerals, ice ( $2.09 \text{ kJ m}^{-3} \text{ }^\circ\text{C}^{-1}$ ), and unfrozen water ( $4.18 \text{ kJ m}^{-3} \text{ }^\circ\text{C}^{-1}$ ), respectively.  $L$  is the volumetric latent heat of fusion for ice ( $334.56 \text{ kJ m}^{-3}$ ). In Equation 6, the first term refers to the (sensible) heat capacity of the soil and the second term is the apparent capacity (latent heat) of the soil.

The change trend of the latent heat capacity can be roughly determined by the typical power-curve relationship between unfrozen water and temperature as was suggested by Anderson and Tice (1973):

$$W_u = a \cdot T^{-b} \quad (8)$$

where  $W_u$  is the unfrozen water content,  $T$  is the absolute value of negative temperature, and  $a$  and  $b$  are the empirical coefficients according to the soil. The curve of unfrozen water indicates that the primary conversion of ice into water happens when the temperature is above  $-3$  or  $-2$   $^\circ\text{C}$ , especially when permafrost temperature is close to  $0$   $^\circ\text{C}$  (Fig. 8, part a).

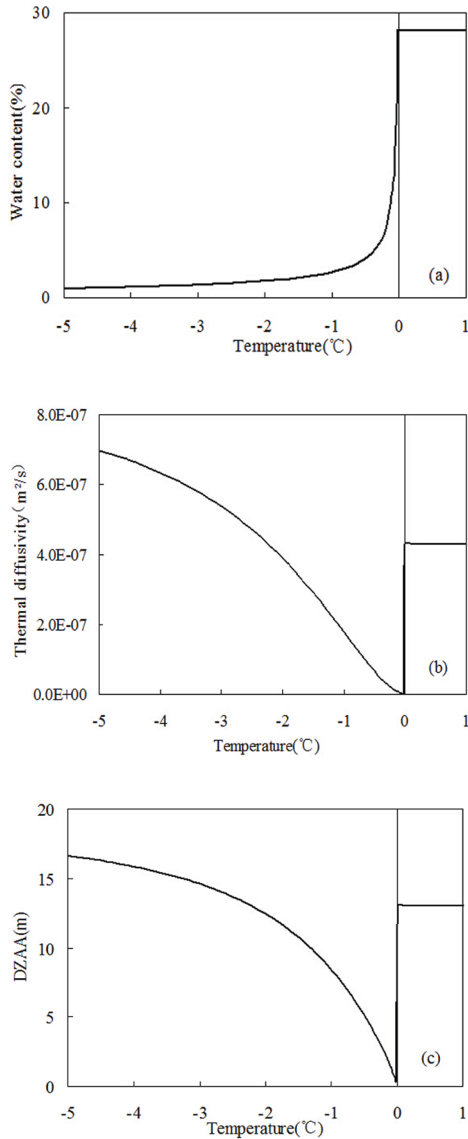


**FIGURE 8.** Variations of (a) the water content, (b) the thermal diffusivity, and (c) the DZAA with temperature for given soil (sandy soil with 28% gravimetric water content).

Using these theoretical formulations, if the permafrost is assumed uniform at different depths and unfrozen water does not move within the permafrost, the change trends of the thermal diffusivity and the DZAA can be analyzed by these formulas based on given values of  $W$ ,  $a$ ,  $b$ ,  $\lambda_m$  and  $C_{sf}$ . In this research, we choose a typical sandy soil with 28% gravimetric water content as the representative soil type on the QTP to simulate the change trend of the permafrost thermal profile and the DZAA. The values for  $a$ ,  $b$ ,  $\lambda_m$ , and  $C_{sf}$  are 2.7, 0.6,  $1.67 \text{ W m}^{-1} \cdot \text{°C}^{-1}$  and  $1.87 \text{ kJ} \cdot \text{m}^{-3} \cdot \text{°C}^{-1}$ , respectively (Xu et al., 2001).

From Figure 8, part a, it is evident that with the increase of ground temperature, unfrozen water content increases sharply when soil temperatures are greater than  $-1 \text{ °C}$  and the main ice-water phase change occurs when the temperature is close to  $0 \text{ °C}$ . Previous work has shown that when water changes to ice, its conductivity increases fourfold, its mass heat capacity decreases by

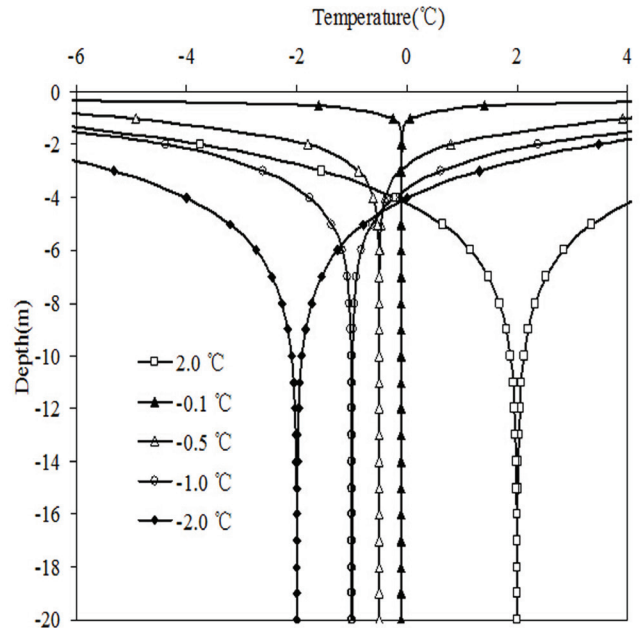


**FIGURE 9.** Simulated thermal trumpet curves for five scenarios with different temperature conditions.

half, and it releases heat equivalent to that required to raise the temperature of an equal volume of rock by about  $150 \text{ °C}$  (Gold and Lachenbruch, 1973). Hence, when the permafrost temperature is close to  $0 \text{ °C}$ , the heat capacity of frozen soil,  $C_f$ , is quite minor compared to the latent heat capacity, and the thermal diffusivity is dominated by the latent heat capacity. The latent heat effects dominate the changes in thermal diffusivity, the DZAA, and the amplitude of the temperature wave in the permafrost. Figure 8, parts b and c, show the changes in thermal diffusivity and the DZAA in the permafrost. It is also evident that when soil temperature is  $-3 \text{ °C}$ , the DZAA is about 15 m, and then it decreases steadily with the increase of soil temperature. When the soil temperature is higher than  $-1 \text{ °C}$ , the DZAA decreases sharply from about 8.5 m to about 0 m at  $0 \text{ °C}$ . For the same soil type, following Equation 2, the amplitudes of the temperature wave at different depths were calculated for five soil temperature scenarios (Fig. 9). It can be seen that the thermal trumpet curves are narrower and the DZAA is shallow when the temperature is close to  $0 \text{ °C}$ , and vice versa. In nonpermafrost soil, since there is no ice-water phase change and thus no latent heat effects, both the thermal diffusivity and the DZAA are stable and the thermal trumpet curves are wide. These simulation results are similar to the observational results along the QXHW.

The theoretical and numerical analyses presented above clearly show that permafrost thermal profiles will inevitably be adjusted when ground temperature increases. The temperature-dependent adjustment in permafrost has important effects on the permafrost degradation on the QTP for climate warming scenarios. It is evident that the decrease of the DZAA will result in the increase of the temperature gradient in the shallower layer and thus is an important influence on ground heat flux in the permafrost. In summer, the temperature gradient remains negative (the overlying soils were warmer than the underlying soils) in the permafrost region above the DZAA. Absolute value of the temperature gradient is very large at those sites with small DZAA, but is relatively small at those sites with large DZAA, as expected. For example, on the warmest date, average absolute value of the temperature

gradient is about  $4.1\text{ }^{\circ}\text{C m}^{-1}$  between 0 m to DZAA at QTB4, but it is about  $0.03\text{ }^{\circ}\text{C m}^{-1}$  in the lower section. The former is almost 136 times the latter. The large temperature gradient in the shallow layer implies that a greater portion of the annual energy exchange between permafrost and atmosphere was consumed by the latent heat effects in the upper permafrost, which will promote the downward degradation of permafrost and result in large ALT. The small DZAA can well explain why the ALT has been increasing faster in warm permafrost regions (e.g., Wu and Zhang, 2010; Zhao et al., 2010).

In winter, the temperature gradient remains positive (the overlying soils are colder than the underlying soils) in permafrost. The temperature gradients above the DZAA are large at those sites with small DZAA and are relatively small at those sites with larger DZAA. The large temperature gradient in the upper layer has attenuated the cooling process into the deep permafrost. The heat flux into the permafrost will be reduced and geothermal heat will contribute to the thawing at the base of permafrost, which will promote upward degradation of permafrost in these warm sites. Hence, the decrease of the DZAA will promote both the downward and upward degradation of permafrost. In the QTP, both the downward degradation and the upward degradation of permafrost were observed in the past several decades in the QTP. Jin et al. (2006) estimated that along the QXHW, the upward degradation has been proceeding at annual rates of 12 to 30 cm during the last quarter century in some warm permafrost regions, which exceed the 4 cm per year for the past 20 years reported for the discontinuous permafrost zone in subarctic Alaska (Osterkamp and Romanovsky, 1997; Osterkamp, 2003; Jin et al., 2006). The difference of permafrost temperature regime and the DZAA is likely the primary reason for this difference.

From the observational results and above numerical analyses, it can be concluded that there is a causal relationship between permafrost thermal conditions and the decrease of the DZAA. The majority of permafrost on the QTP is undergoing internal thaw and it remains in an endangered state. It is the latent heat effects that result in different responses in permafrost with different thermal condition. The slow warming rate and rapid increase of the ALT were primarily due to the permafrost thermal regime. According to the current climate warming, when the latent heat effect finally becomes weak, permafrost on the QTP will eventually collapse. The current permafrost thermal regime change on the QTP is very likely to mirror all the permafrost in the northern hemisphere, and the research results of high-temperature permafrost on the QTP will help us understand the change of cold permafrost in the future.

## Conclusion

Based on the observation results and numerical analysis, this work suggests that permafrost temperature regimes, whether cold or warm, not only have an important implication on the warming trend of the permafrost, but also have significant impact on the distribution of vertical profile of ground temperature. Continuous data obtained from 17 monitoring sites on the QTP show that permafrost thermal trumpet curves are generally narrow and the DZAAs are generally shallow in warm permafrost regions. The DZAA at more than half monitoring sites is less than 7.0 m and the average value of DZAA is 8.5 m. At three sites where permafrost temperature is close to  $0\text{ }^{\circ}\text{C}$ , the observed DZAAs are less than 4.0 m. In the low-temperature permafrost regions, DZAA is usually deeper than that in warm permafrost regions. It is usually deeper than 10.0 m and the deepest one is about 16.0 m at QTB 16. This research theoretically proved that there is a causal relationship between

permafrost warming and the decrease of the DZAA. Latent heat effects are buffering the increase of permafrost temperature and result in narrow thermal trumpet curves and shallow DZAAs when permafrost temperature is close to  $0\text{ }^{\circ}\text{C}$ . This research suggests that the temperature-dependent adjustments in permafrost will promote both downward and upward degradation of permafrost under climate warming.

## Acknowledgments

This work was supported by a grant from the National Major Scientific Project of China, "Crospheric Change and Impacts Research (2013BA01803)," State Key Laboratory of Crospheric Sciences (SKLCS-ZZ-2012-02-03), the National Natural Sciences Foundation of China (41271086), and the Hundred Talents Program of Chinese Academy of Sciences Grant to Xie Changwei (51Y551831).

## References Cited

- Anderson, D. M., and Tice, A. R., 1973: The unfrozen interfacial phases in frozen soil water systems. In Hadas, A., Swartzendruber, D., Rijtema, P. E., Fuchs, M., and Yaron, B. (eds.), *Physical Aspects of Soil Water and Salts in Ecosystems, Ecological Studies, 4*. New York: Springer, 107–124.
- Brown, J., Hinkel, K. M., and Nelson, F. E., 2000: The Circumpolar Active Layer Monitoring (CALM) Program: Research design and initial results. *Polar Geography*, 24: 165–253.
- Burn, C. R., and Zhang, Y., 2009: Permafrost and climate change at Herschel Island (Qikiqtaruq), Yukon Territory, Canada. *Journal of Geophysical Research*, 114, F02001, doi <http://dx.doi.org/10.1029/2008JF001087>.
- Cheng, G. D., 1983: The mechanism of repeated segregation for the formation of thick-layered ground ice. *Cold Regions Science and Technology*, 8: 57–66.
- Cheng, G. D., 2003: The effect of local factors on spatial distribution of permafrost and its revealing to Qinghai–Xizang Railroad design. *Science in China, Series D*, 33 (6): 602–607.
- Cheng, G. D., and Wu, T. H., 2007: Responses of permafrost to climate change and their environmental significance, Qinghai–Tibet Plateau. *Journal of Geophysical Research*, 112: F02S03, doi <http://dx.doi.org/10.1029/2006JF000631>.
- Christiansen, H. H., Etzelmüller, B., Isaksen, K., Juliussen, H., Farbrot, H., Humlum, O., Johansson, M., Ingeman-Nielsen, T., Kristensen, L., Hjort, J., Holmlund, P., Sannel, A. B. K., Sigsgaard, C., Åkerman, H. J., Foged, N., Blikra, L. H., Pemosky, M. A., and Ødegård, R. S., 2010: The thermal state of permafrost in the Nordic area during the International Polar Year 2007–2009. *Permafrost and Periglacial Processes*, 21: 156–181.
- Du, J., 2003: Asymmetric change of maximum and minimum temperature in Tibetan plateau from 1971–2000. *Journal of Applied Meteorological Science*, 14: 437–444.
- Frauenfeld, O. W., Zhang, T. J., and Barry, R. G., 2004: Interdecadal changes in seasonal freeze and thaw depths in Russia. *Journal of Geophysical Research*, 109: D05101, doi <http://dx.doi.org/10.1029/2003JD004245>.
- Gold, L. W., and Lachenbruch, A. H., 1973: Thermal conditions in permafrost: a review of North American literature. In Proceedings, 2nd International Permafrost Conference, 13–28 July 1973, Yakutsk, U.S.S.R., National Academy of Sciences, Washington, DC (1973), pp. 3–25 North American contribution.
- Goodrich, L. E., 1976: *A Numerical Model for Assessing the Influence of Snow Covers on the Ground Thermal Regime*. Ph.D. thesis, Montreal, McGill University.
- Haerberli, W., Cheng, G., Gorbunov, A. P., and Harris, S. A., 1993: Mountain permafrost and climatic change. *Permafrost and Periglacial Processes*, 4: 165–174.

- Hinzman, L. D., Bettez, N. D., Bolton, W. R., et al. 2005: Evidence and implications of recent climate change in northern Alaska and other Arctic regions. *Climate Change*, 72(3), 251–298.
- Ingersoll, L. R., Zobel, O. J., and Ingersoll, A. C., 1954: *Heat Conduction with Engineering, Geological and Other Applications*. New York: McGraw-Hill, 325 pp.
- Isaksen, K., Sollid, J. L., Holmlund, P., and Harris, C., 2007: Recent warming of mountain permafrost in Svalbard and Scandinavia. *Journal Geophysical Research*, 112: F02S04, doi <http://dx.doi.org/10.1029/2006JF000522>.
- Jin, H. J., Zhao, L., and Wang, S. L., 2006: Thermal regimes and degradation modes of permafrost along the Qinghai-Tibet Highway. *Science in China Series (D)*, 34(11): 1009–1019.
- Jin, H. J., Sun, L. G., Wang, S. L., He, R. X., Lü, L. Z., and Yu, S. P., 2008: Dual Influences of Local Environmental Variables on Ground Temperatures on the Interior-Eastern Qinghai-Tibet Plateau(I): Vegetation and Snow Cover. *Journal Glaciology and Geocryology*, 30: 535–545.
- Lemke, P., Ren, J. W., Alley, R. B., Carrasco, J., Flato, G., and Fujii, Y., 2007: Observations: changes in snow, ice and frozen ground. In Solomon, S., Qin, D., Manning, M., et al. (eds.), *Climate Change 2007: The Physical Science Basis*. Cambridge and New York: Cambridge University Press, Contribution of Working Group I to the Fourth Assessment Report of the Intergovernmental Panel on Climate Change.
- Lu, L. Z., Jin, H. J., Wang, S. L., et al., 2008: Dual influences of local environmental variables on ground temperatures on the interior-eastern Qinghai-Tibet Plateau (II): sandy layer and surface water bodies. *Journal Glaciology and Geocryology*, 30: 546–555.
- Ma, X. B., 1999: The asymmetric change of maximum and minimum temperature in the Northwest China. *Acta Meteorologica Sinica*, 57: 613–621.
- Nelson, F. E., Shiklomanov, N. I., Hinkel, K. M., and Christiansen, H. H., 2004: The Circumpolar Active Layer Monitoring (CALM) Workshop and the CALM II Program. *Polar Geography*, 28: 253–266.
- Oberman, N. G., and Mazhitova, G. G., 2001: Permafrost dynamics in the northeast of European Russia at the end of the 20th century. *Norwegian Journal Geography*, 55: 241–244.
- Osterkamp, T. E., 2003: A thermal history of permafrost in Alaska. In Proceedings, Eighth International Conference on Permafrost. Zurich: Balkema Publishers, 863–868.
- Osterkamp, T. E., 2005: The recent warming of permafrost in Alaska. *Global Planet Change*, 49: 187–202.
- Osterkamp, T. E., and Romanovsky, V. E., 1997: Freezing of the active layer on the coastal plain of the Alaskan Arctic. *Permafrost and Periglacial Process*, 8: 23–44
- Pang, Q. Q., Zhao, L., Li, S. X., and Ding, Y. J., 2011: Active layer thickness variations on the Qinghai-Tibet Plateau under the scenarios of climate change. *Environment Earth Science*, doi <http://dx.doi.org/10.1007/s12665-011-1296-1>.
- Qiu, G. Q., Liu, J. R., and Liu, H. X., 1994: *Geocryological Glossary*. Lanzhou: Gansu Science Press, 28 pp.
- Riseborough, D. W., 1990: Soil latent heat as a filter of the climate signal in permafrost. In Proceedings, Fifth Canadian Permafrost Conference, Collection Nordicana No. 54, Université Laval, Québec, 199–205.
- Romanovsky, V. E., Drozdov, D. S., Oberman, N. G., Malkova, G. V., Kholodov, A. L., Marchenko, S. S., Moskalenko, N. G., Sergeev, D. O., Ukraintseva, N. G., Abramov, A. A., Gilichinsky, D. A., and Vasiliev, A. A., 2010b: Thermal state of permafrost in Russia. *Permafrost and Periglacial Processes*, 21: 136–155.
- Romanovsky, V. E., Smith, S. L., and Christiansen H. H., 2010a: Permafrost thermal state in the polar northern hemisphere during the International Polar Year 2007–2009: a synthesis. *Permafrost and Periglacial Processes* 21: 106–116
- Smith, S. L., and Brown, J., 2009: T7 Permafrost: permafrost and seasonally frozen ground. *Global Terrestrial Observing System, GTOS*, 62: 19 pp.
- Smith, M.W. and Riseborough, D.W., 1985: The sensitivity of thermal predictions to assumptions in soil properties. Proceedings of the Fourth International Conference on Ground Freezing, Sapporo, Japan, Vol. I, pp. 17–23. Balkema.
- Smith, S. L., Wolfe, S. A., Risborough, D. W., and Nixon, F. M., 2009: Active layer characteristics and summer climate indices, Mackenzie Valley, Northwest Territories, Canada. *Permafrost Periglacial Process*, 20: 201–220.
- Smith, S. L., Romanovsky, V. E., Lewkowicz, A. G., Burn, C. R., Allard, M., Clow, G. D., Yoshikawa, K., and Throop, J., 2010: Thermal state of permafrost in North America: a contribution to the International Polar Year. *Permafrost and Periglacial Processes*, 21: 117–135.
- Walsh, J. E., Anisimov, O., Hagen, J. M., et al., 2005: Cryosphere and hydrology. In Symon, C., Arris, L., and Heal, B. (eds.), *Arctic Climate Impacts Assessment, ACIA*. Cambridge: Cambridge University Press, 183–242.
- Wang, S., Zhao, L., and Li, S. X., 2002: Interaction between permafrost and desertification on the Qinghai-Tibet Plateau. *Journal of Desert Research*, 22(1): 33–39 (in Chinese with English abstract).
- Williams, P. J., and Smith, M. W., 1989: *The Frozen Earth: Fundamentals of Geocryology*. New York: Cambridge University Press.
- Wu, Q. B., and Zhang, T., 2008: Recent permafrost warming on the Qinghai-Tibetan Plateau. *Journal of Geophysical Research*, 113: D13108, doi <http://dx.doi.org/10.1029/2007JD009539>.
- Wu, Q. B., and Zhang, T., 2010: Changes in active layer thickness over the Qinghai-Tibetan Plateau from 1995 to 2007. *Journal of Geophysical Research*, 115: D09107, doi <http://dx.doi.org/10.1029/2009JD012974>.
- Wu, Q. B., Zhang, T. J., and Liu, Y. Z., 2010a: Permafrost temperatures and thickness on the Qinghai-Tibet Plateau. *Global and Planetary Change*, 72: 32–38.
- Wu, J. C., Sheng, Y., and Wu, Q. B., 2010b: Processes and mode of permafrost degradation on the Qinghai-Tibet Plateau. *Science in China Series (D)*, 53: 150–158.
- Xie, C. W., Zhao, L., Wu, T. H., and Dong, X. C., 2012: Changes in the thermal and hydraulic regime within the active layer in the Qinghai-Tibet Plateau. *Journal of Mountain Science*, 9: 483–491.
- Xu, X. Z., Wang, J. C., and Zhang, L. X., 2001: *Physics of frozen soil*. Beijing: Science Press.
- Zhang, T. Frauenfeld, O. W., Serreze, M. C., Etringer, A., Oelke, C., McCreight, J., Barry, R. G., Gilichinsky, D., Yang, D., Ye, H., Ling, F., and Chudinova, Svetlana, 2005: Spatial and temporal variability in active layer thickness over the Russian Arctic drainage basin. *Journal of Geophysical Research*, 110: D16101, doi <http://dx.doi.org/10.1029/2004JD005642>.
- Zhao, L., Wu, Q. B., Marchenko, S. S., and Sharkhuu, N., 2010: Thermal state of permafrost and active layer in Central Asia during the International Polar Year. *Permafrost and Periglacial Process*, 21: 198–207.
- Zhou, Y. W., Guo, D. X., and Qiu, G. Q., 2000: *Geocryology in China*. Beijing: Science Press.

MS accepted June 2015